TISSUE ENGINEERING: Part A
Volume 16, Number 12, 2010

DOI: 10.1089/ten.tea.2009.0786

Genetically Modified Mesenchymal Stem Cells Induce Mechanically Stable Posterior Spine Fusion

Dima Sheyn, M.Sc.,[1] Martin Rüthemann, M.Sc.,[2] Olga Mizrahi, B.Sc.,[1] Ilan Kallai, B.Sc.,[1] Yoram Zilberman, D.M.D., Ph.D.,[1] Wafa Tawackoli, Ph.D.,[3] Linda E.A. Kanim, M.Sc.,[4] Li Zhao, M.D.,[4] Hyun Bae, M.D.,[4] Gadi Pelled, D.M.D., Ph.D.,[1,3] Jess G. Snedeker, Ph.D.,[2,5] and Dan Gazit, D.M.D., Ph.D.[1,3]

Most spine fusion procedures involve the use of prosthetic fixation devices combined with autologous bone grafts rather than biological treatment. We had shown that spine fusion could be achieved by injection of bone morphogenetic protein-2 (BMP-2)-expressing mesenchymal stem cells (MSCs) into the paraspinal muscle. In this study, we hypothesized that posterior spinal fusion achieved using genetically modified MSCs would be mechanically comparable to that realized using a mechanical fixation. BMP-2-expressing MSCs were injected bilaterally into paravertebral muscles of the mouse lumbar spine. In one control group BMP-2 expression was inhibited. Microcomputed tomography and histological analyses were used to evaluate bone formation. For comparison, a group of mouse spines were bilaterally fused with stainless steel pins. The harvested spines were later tested using a custom four-point bending apparatus and structural bending stiffness was estimated. To assess the degree to which MSC vertebral fusion was targeted and to quantify the effects of fusion on adjacent spinal segments, images of the loaded spine curvature were analyzed to extract rigidity of the individual spinal segments. Bone bridging of the targeted vertebrae was observed in the BMP-2-expressing MSC group, whereas no bone formation was noted in any control group. The biomechanical tests showed that MSC-mediated spinal fusion was as effective as stainless steel pin-based fusion and significantly more rigid than the control groups. Local analysis showed that the distribution of stiffness in the MSC-based fusion group was similar to that in the steel pin fusion group, with the majority of spinal stiffness contributed by the targeted fusion at L3–L5. Our findings demonstrate that MSC-induced spinal fusion can convey biomechanical rigidity to a targeted segment that is comparable to that achieved using an instrumental fixation.

Introduction

Low back pain is the most common cause of disability in people younger than 45 years. It accounts for 8 million physician visits and 89 million lost work days per year,[1] and it incurs an estimated cost of up to $50 billion annually.[2] Low back pain is caused by intervertebral disc degeneration and other pathological conditions such as spondylosis, scoliosis, spondylolisthesis, tumor, infection, and posttraumatic fracture.[3] Fusion of two or more adjacent vertebrae is commonly performed to treat these debilitating conditions, and >250,000 such procedures are performed annually in the United States alone.[4] The complication rates in these procedures, although low, increase with patient age and reach 12% in patients older than 75 years.[5] Procedures involving the application of bone grafts harvested from the iliac crest reportedly lead to adverse complications in 10%–35% of cases.[6,7] Another widely used treatment includes the implantation of metal cages containing recombinant bone morphogenetic protein-2 (BMP-2). High-dose recombinant human BMP-2 (rhBMP2) has been found to cause pseudarthroses,[8,9] various infections,[10] ectopic bone formation that cause neural compression,[11] and abdominal bone growth.[12] In osteoporotic compression fractures of the spine, the use of instrumental fixation to achieve spinal fusion has a high failure rate due to low bone mass; when this procedure is combined with vertebral augmentation involving biomaterials such as poly(methyl methacrylate) (PMMA), a significant modulus mismatch with adjacent vertebrae may occur, leading to increased stress at the augmented–nonaugmented junction.[13]

Efforts have been made to develop an injectable biological agent that would induce spine fusion without the need for

[1]Skeletal Biotech Laboratory, Faculty of Dental Medicine, The Hebrew University of Jerusalem, Jerusalem, Israel.
[2]Department of Orthopedics, University of Zurich, Balgrist, Zurich, Switzerland.
[3]Department of Surgery and Cedars-Sinai Regenerative Medicine Institute (CS-RMI), Cedars Sinai Medical Center, Los Angeles, California.
[4]Spine Institute, Cedars Sinai Medical Center, Los Angeles, California.
[5]Department of Mechanical Engineering, ETH Zurich, Zurich, Switzerland.

bone grafts and synthetic implants. Such a solution would avoid open surgery and lengthy hospitalization, which is largely responsible for the high costs of treating lower back pain.[14] It would also reduce the risks of open surgery, such as respiratory and cardiac complications, because such an injection can be given using a local anesthetic agent. Finally, if fusion is not achieved, additional injections can be administered without subjecting the patient to multiple surgical procedures.

Direct delivery of osteogenic genes to induce spine fusion has been described in several studies.[4,15] Another attractive biological approach used to induce fusion includes the injection of genetically modified mesenchymal stem cells (MSCs).[16–19] We previously demonstrated that MSCs overexpressing a BMP gene could be effectively used to induce spine fusion in a mouse model.[20,21] The BMP gene can be introduced into a cell in a variety of ways, including viral[22,23] and nonviral methods.[21,24] MSCs can be isolated from various adult tissues, such as bone marrow and adipose tissue,[25] following common procedures such as liposuction.

We have explored structural,[20,21] nanomechanical, and nanostructural properties of bone tissue induced by engineered MSCs, and showed that intrinsic biomechanical properties may depend on the injection site.[26,27] However, to date, no one has reported whether the bone mass generated by engineered MSCs can indeed lead to mechanical stabilization, which is the prime goal of spine fusion.

In this study we injected BMP-2-engineered MSCs into the paraspinal muscles of mice to achieve lumbar spine fusion. Five weeks after injection, at which point prominent bone masses had formed, we tested the bending rigidity of the fused lumbar spines and compared our findings with those in spines fused with stainless steel pins or injected with MSCs that did not express BMP-2.[28] We also analyzed the structural properties of the newly formed bone using microcomputed tomography (μCT). Our results indicated that MSC-mediated spinal fusion was as rigid as stainless steel pin-based fusion and was significantly more rigid than any fusion attained in the control groups. Interestingly, these mechanical results were achieved even though the newly formed bone had lower bone volume density and mineral density than the host vertebrae. Finally, by performing an immunohistochemical analysis we were able to identify implanted MSCs in the new bone that fused the vertebrae.

This is the first report demonstrating that injections of BMP-2-engineered MSCs can lead to biomechanically robust spine fusion. The results of this study constitute another step toward a novel biological solution for the minimally invasive treatment of lower back pain.

Materials and Methods

Generation of a genetically engineered MSC line

Genetic engineering of MSCs to express BMP-2 in a doxycycline (DOX)-inducible system has been described elsewhere.[28] Briefly, cells from the C3H10T1/2 MSC line were transfected with a ptTATop-BMP-2 plasmid vector that encodes for both the tetracycline transactivator and BMP-2 cDNAs. In addition, the cells were infected with a retrovirus encoding for the β-galactosidase (β-*Gal*) reporter gene, as previously reported,[28] so that we could track the cells *in situ*. Expression of BMP-2 can be shut off in the presence of DOX, a homolog of tetracycline, or turned on in DOX's absence. We previously showed that this MSC line is capable of inducing bone formation in ectopic and orthotopic implantation sites.[20,28]

Cell culture

Cells were cultured in 140-mm culture plates in a complete growth medium (Dulbecco's modified Eagle's medium containing 10% fetal bovine serum, 2 mM L-glutamine, 100 U/mL penicillin, and 100 U/mL streptomycin; Biological Industries, Beit Haemek, Israel) in a 5% CO_2/95% air atmosphere at 37°C. DOX (1 μg/mL) was added to the medium to prevent cell differentiation before implantation. Before the *in vivo* studies commenced, the cells were trypsinized and centrifuged at 300 *g* and 4°C for 5 min. The cells were counted using the Trypan blue exclusion test and separated into aliquots of 5×10^6 cells.

In vivo *cell injection*

All procedures used in this study were approved by the Hebrew University institutional animal care and use committee. Cohorts of 10-week-old female C3H/HeN mice were anesthetized by intraperitoneal injection of a xylazine–ketamine mixture (3.3 mg/kg xylazine and 100 mg/kg ketamine). Aliquots of 5×10^6 MSCs were suspended in 50 μL fibrin gel (Tisseel; Baxter, Vienna, Austria) and injected into the lumbar paravertebral muscle in a manner previously described[20,21] and illustrated in Figure 1. Each mouse received two injections, one injection on each side. The experimental group (nine mice), denoted as the MSC/−DOX group, received injections of BMP-2-expressing MSCs followed by a normal diet of food and water. The control cohort (seven mice), denoted as the MSC/+DOX group, also received injections of BMP-2-expressing MSCs but were given DOX in their drinking water (0.5 mg/mL) to shut off BMP-2 expression. Another control group (seven mice), known as the FG Only group, received injections containing only fibrin gel. The mice were housed in a specific pathogen-free animal facility. After 5 weeks the mice were euthanized by an overdose of pentobarbital (120 mg/kg i.p.) after which their

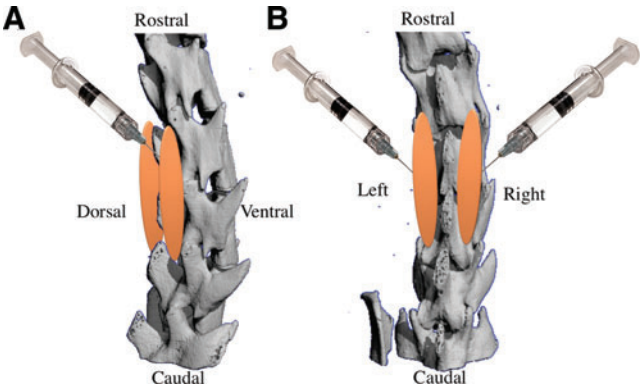

FIG. 1. This diagram demonstrates the site and the direction of the stem cell injection to the paraspinal muscle in lateral (**A**) and posterior (**B**) view. Orange color represents the new bone formation in the site of stem cells injection. Color images available online at www.liebertonline.com/ten.

spines were harvested, wrapped in saline-soaked gauze, and frozen in −20°C. Some spines were stored without fixation in −20°C, thawed for a few hours in phosphate-buffered saline (PBS) for μCT scanning, and frozen again until subjected to biomechanical tests. Other spines destined for histological analysis were fixed in 4% formalin.

Microcomputed tomography

To evaluate volumes of bone formation and structural parameters, each spine was scanned using a desktop cone-beam μCT scanner (μCT 40; Scanco Medical AG, Bassersdorf, Switzerland). Micro-tomographic slices were acquired at 1000 projections and reconstructed at a spatial nominal resolution of 16 μm. Newly formed bone was separated from native bone by manual contouring. As a reference for mature native bone, we used posterior portions of mouse lumbar vertebrae contoured in the same manner (Native Spine group). Using direct three-dimensional (3D) morphometry for newly formed bone and control tissue, we determined the following morphometric indices: (a) total bone volume (TV) in cubic millimeters, which included bone and soft tissue regions; (b) volume of mineralized bone tissue (BV) in cubic millimeters; (c) bone volume density (BVD), which was calculated as the BV/TV ratio; (d) bone mineral density (BMD; mg hydroxyapatite (HA)/cm^3) derived from the projectional image and calculated based on calibration with commercially available Micro-CT phantom containing H_2KPO_4 (Scanco Medical AG); (e) average bone thickness (BT) in millimeters; (f) degree of anisotropy (DA), which was determined from the ratio of maximal to minimal radii of the mean intercept length of the ellipsoid; and (g) connectivity density (Conn-Den; mm^{-3}).[29,30] The extent of the fusion and the number of vertebrae that were fused were determined manually by examining coronal and lateral sections of 3D images.

Biomechanical assays

Mouse spine preparation. All muscle and soft tissue surrounding the spines were removed, taking care to leave the joint capsules and spinal ligaments intact. To simulate the posterolateral spinal fusion that can be achieved using metal implants, the spines of seven 10-week-old C3H/HeN mice were fixed bilaterally between L-3 and L-5 by using 0.8-mm stainless steel pins. Additional specimens ($n = 7$) were collected and tested as intact spines (Native Spine group).

Assessing lumbar spine rigidity in four-point bending. Loading assays were performed on an L2–6 segment for all groups, the analog of the human L1–5 segment. To determine the parameters for testing, intact spines were nondestructively tested using a custom-made four-point bending apparatus and a universal test machine (Zwick 1456, Ulm, Germany). As the extremely low bending stiffness of the normal murine spine precluded the use of potting materials, we relied only on the natural curvature of the spine and gravity to mount specimens within the test apparatus. The exterior support span was set to 15.3 mm, thus supporting the L6–S1 and L1–L2 junctions. An interior support span of 4.5 mm was centered with respect to the outer span. Spines were subjected to five loading cycles of 0.40 N at a rate of 0.10 N/s, which resulted in an approximate bending moment of 1.1 N mm. Load–displacement data from the final cycle and the test geometry were then used to generate an approximate structural bending stiffness (elastic modulus multiplied by area moment of inertia [EI]).[31,32]

Assessing local rigidity of fused and adjacent segments. A localized analysis of bending stiffness in individual spine segments was performed by analyzing moment-induced changes in the spine's radius of curvature. Four-point bending was performed, as described earlier, while obtaining lateral images of the spine with the aid of a high-resolution digital video camera (Basler A602f, Ahrensburg, Germany). Semiautomated image postprocessing was implemented to detect the contour of the anterior spine and to fit a fourth-order polynomial curve to the contour. The bending stiffness of a designated section of the lumbar spine was then derived from the applied bending moment and the radius of the segment curvature.[33]

Histological analysis

Harvested specimens were fixed in 4% formalin for 24 h, decalcified by soaking in 0.5 M ethylenediaminetetraacetic acid solution (pH = 7.4) for 2 weeks, and dehydrated by passing through an increasing-grade series of ethanol baths, and embedded in paraffin. Five-micron-thick sections were cut from each paraffin block with the aid of a motorized microtome (Leica Microsystems, Nussloch, Germany). Hematoxylin and eosin (H&E) and bone matrix-specific Masson trichrome stain were applied to tissue sections as previously reported.[34]

Immunohistochemical staining for β-galactosidase

An immunohistochemical assay (HISTOSTAIN KIT, Catalog No. 956143; Zymed Laboratories, South San Francisco, CA) was performed on paraffin sections of fused spines to detect expression of the β-*Gal* reporter gene by the engineered MSCs.[28] Sections of tissue were deparaffinized by applying xylene, rehydrated by bathing in a descending-grade series of ethanol, and rinsed with double distillered water (DDW). Endogenous peroxidase activity was removed by treatment with 0.1% H_2O_2. A primary antibody that reacts with rabbit β-*Gal* (ab616-100; Abcam, Cambridge Science Park, Cambridge, United Kingdom) was diluted 1:750 in 3% PBS/bovine serum albumin and applied to the slides for 1 h at room temperature. After incubation with the primary antibody, the slides were rinsed in PBS and a secondary rabbit anti-mouse immunoglobulin G-antibody (biotin-conjugated; Zymed Laboratories) was applied to the slides at room temperature for 30 min. After they had been washed with PBS, the slides were incubated with horseradish peroxidase conjugated to streptavidin and then stained with 3-amino-9-ethylcarbazole dye. The slides were counterstained with hematoxylin, washed, mounted with GVA (Zymed Laboratories), and observed with the aid of light microscopy.

Statistical analysis

All mean values in the Results section and figures are displayed with their standard errors. Statistical tests for significance were performed using the two-tailed Student's *t*-test, and the minimal criterion for significance was determined to be a probability level <0.05.

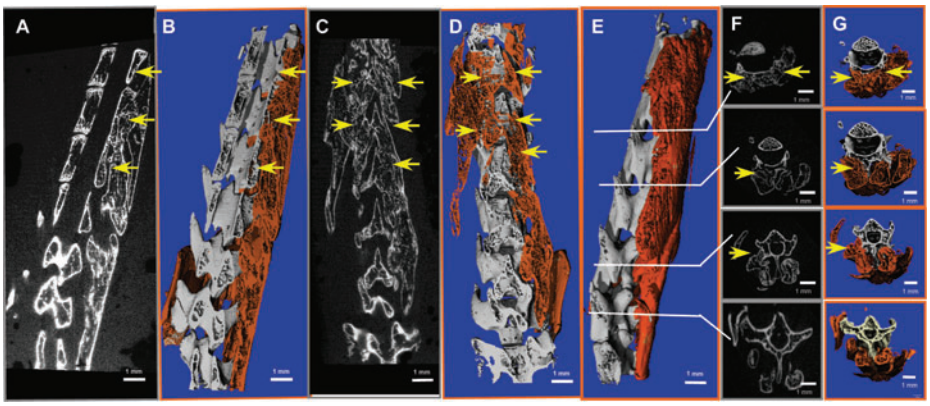

FIG. 2. Spinal fusion imaging using μCT. Mouse spines were harvested 5 weeks after MSCs genetically engineered to express BMP-2 were injected bilaterally into the paravertebral muscles. New bone mass was contoured manually and is represented by the orange regions in the 3D images (**B, D**). Yellow arrows indicate fusion sites (**A–G**). Sagittal (**A, B**), coronal (**C, D**), and lateral (**E**) 3D reconstructed image of a representative spine were made using Scanco software. Axial sections of the spine are shown in 2D (**F**) and 3D (**E**) images. μCT, microcomputed tomography; MSC, mesenchymal stem cells; BMP-2, bone morphogenetic protein-2; 3D, three-dimensional. Color images available online at www.liebertonline.com/ten.

Results

μCT-based analysis of newly formed spine fusion

In this study MSCs that had been genetically engineered to express BMP-2 were suspended in fibrin gel, and the suspension was then injected into the paravertebral muscles of 10-week-old C3H/HeN mice to achieve posterolateral spinal fusion. Five weeks after injection, the mouse spines were harvested and evaluated using μCT. New bone formation was evident in all mice that received MSCs, but no DOX was added to their drinking water (MSC/−DOX group). No bone formation was detected in the control groups (MSC/+DOX and FG Only groups); thus, complete μCT analysis was only undertaken for the MSC/−DOX group. Results showed that an intervertebral bridge of new bone mass had formed (Fig. 2), fusing 2.4 ± 0.4 vertebrae per injection ($n = 18$) and 3.1 ± 0.6 vertebrae per mouse ($n = 9$). The sites of fusion between the new bone mass and the native vertebrae numbered 2.3 ± 0.4 per injection ($n = 18$). All counts of fusion sites were made by evaluating 3D images and confirmed by evaluating two-dimensional images. The new bone mass formed along the spine, spanning adjacent segments; however, not all segments were fused (Fig. 2).

To evaluate the structural parameters of the newly formed bone masses, we compared them with posterior portions of intact native vertebrae (Fig. 3). In the MSC/−DOX group the TV of newly formed bone (which includes cavities in the tissue) was $132.5 \pm 8.4\,mm^3$ ($n = 9$), and the actual bone volume (BV) for the newly formed mass was $44.7 \pm 3.7\,mm^3$. The BVD (calculated as BV/TV) in the MSC/−DOX group

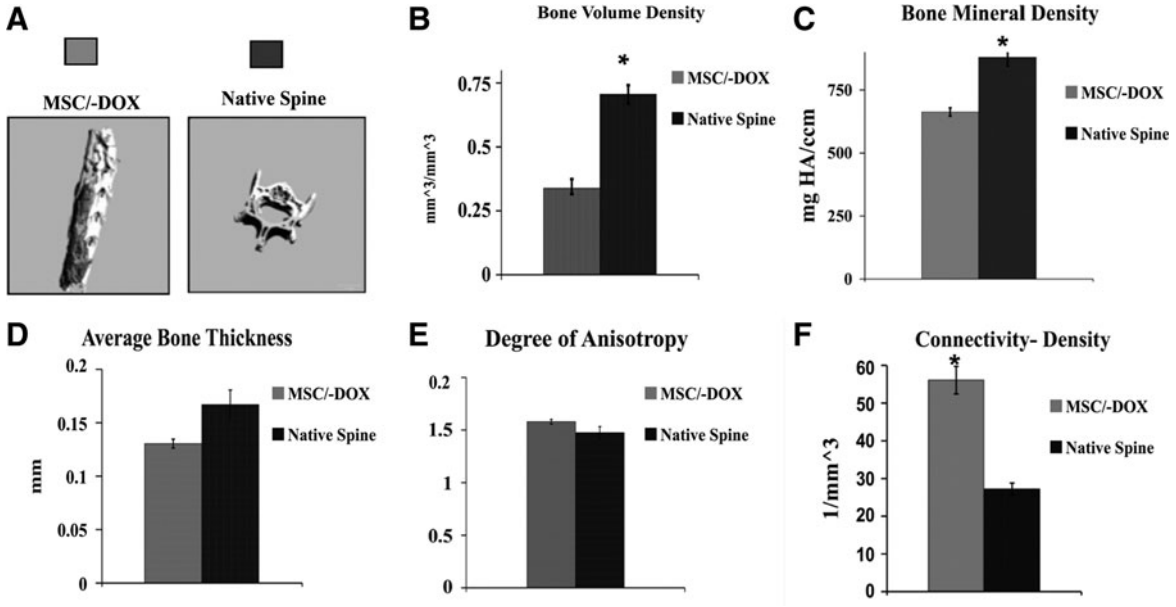

FIG. 3. Quantitative μCT analysis of new bone structural properties (MSC/−DOX group) compared to the posterior portions of intact vertebrae (Native Spine group). (**A**) μCT reconstructed images. (**B–F**) Graphs showing bone structure parameters: bone volume density calculated as the ratio between bone volume and total tissue volume (**B**); bone mineral density (**C**); average bone thickness (**D**); connectivity density (**E**); and degree of anisotropy (**F**). Bars indicate SE, $^*p < 0.05$. MSC/−DOX group $n = 9$; Native Spine group $n = 3$. DOX, doxycycline; SE, standard error; HA, hydroxyapatite.

was 0.34 ± 0.02, whereas that in the control vertebrae (Native Spine group) was much higher: 0.77 ± 0.03 ($n = 3$, $p < 0.05$). The BMD in the MSC/−DOX group was 663 ± 16 mg HA/cm^3 ($n = 9$), whereas the BMD in the Native Spine group was 880 ± 35 mg HA/cm^3 ($n = 3$, $p < 0.05$). The average BT parameter indicates the solidness of newly formed bone.[29] The average thickness of newly formed bone in the MSC/−DOX group was 0.13 ± 0.01 mm ($n = 9$); the average thickness of the control vertebrae (Native Spine Group) was slightly higher, 0.17 ± 0.01 mm ($n = 3$), but the difference was not statistically significant. The parameter of Conn-Den is used to evaluate to what degree the bone is branched and porous at its structure. The fusion mass in the MSC/−DOX group had a Conn-Den value of $56.1 \pm 3.7\,\text{mm}^{-3}$ ($n = 9$), whereas the control vertebrae (Native Spine group) had a value of only $27.3 \pm 1.5\,\text{mm}^{-3}$ ($n = 3$, $p < 0.05$). There was no significant difference between the MSC/−DOX group and the Native Spine group with respect to the DA, another structural parameter. In the MSC/−DOX group the DA in the fusion mass was 1.58 ± 0.02 ($n = 9$), and in the Native Spine group it was 1.47 ± 0.05 ($n = 3$).

Biomechanics of spine fusion

To evaluate the segmental stabilization achieved by posterolateral spinal fusion using genetically engineered MSCs, biomechanical loading tests were performed. We performed loading tests on spines harvested from 10-week-old C3H/HeN mice that had undergone different treatments—injections of BMP-2-expressing MSCs with no DOX added (MSC/−DOX group); spinal fusion performed using stainless steel pins bilaterally through L3–L5 (SSP group); injections of BMP-2-expressing MSCs with the addition of DOX (MSC/+DOX control group); injections of fibrin gel without MSCs (FG Only control group)—or on intact native spines (Native Spine group) (Fig. 4A). The two first groups (containing nine and seven mice, respectively) shared similar values of spinal rigidity and high values of spinal bending modulus (EI, in N/mm^3), which were significantly higher than values found in the control groups (Fig. 4B). The rigidity parameters of each control group were similar to those in the Native Spine group.

To determine which region of the spine contributed the most to rigidity of the lumbar segment, the distribution of spinal stiffness between different spine levels was quantified (Fig. 5). In spines fused using MSCs the majority of spinal stiffness came from the L3–L5 segment, whereas the other segments (L2–L3 and L5–L6) showed little contribution. As expected, similar results were seen in spines fused using stainless steel pins, with the majority of the stiffness oriented in L3–L5 fused segments. The distribution of stiffness in native spines was much more evenly dispersed (Fig. 5).

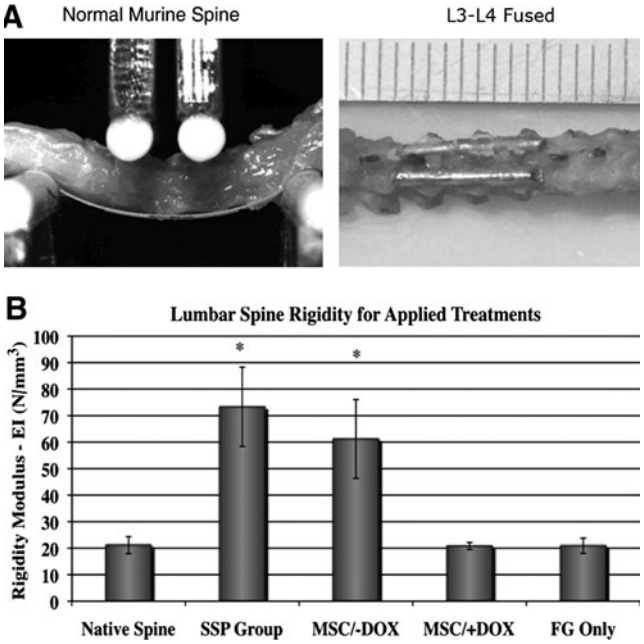

FIG. 4. Lumbar spine rigidity evaluated by opto-mechanical tests. (**A**) Native murine spine subjected to loading tests (on the left) and an image of fused murine spine using bilateral stainless steel is shown on the right. (**B**) Lumbar spine rigidity comparison is shown for spines groups with different treatments. Bars indicate SE ($n = 7$ in each group). SSP group: spinal fusion performed using stainless steel pins; FG Only group: control group received injections containing only fibrin gel. *$p < 0.05$.

Histological analysis

Standard H&E and bone matrix-specific Masson trichrome stains were applied to tissue to examine the morphological characteristics of the newly formed bone masses. The histological sections demonstrated a large area of endochondral bone formation containing a focus of cartilage surrounded by new bone trabeculae. Areas containing bone marrow were evident as well. The new bone tissue was fused to the posterolateral aspect of the mouse vertebrae (Fig. 6A, B).

Contribution of engineered MSCs to new bone formation

An immunohistochemical assay for detection of cells that express β-*Gal* was performed to evaluate the contribution of

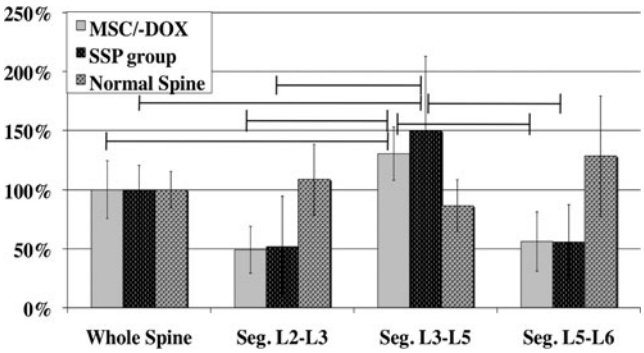

FIG. 5. Segment contributions to total lumbar spine rigidity. Distribution of spinal rigidity is shown for the following segments of the lumbar spine: L1–2, L2–4, and L4–5. The rigidity of each segment is normalized for the rigidity of the entire lumbar spine and shown in percentages. The distribution of rigidity is shown for spines after injection of MSCs genetically engineered to express bone morphogenetic protein-2 (MSC/−DOX group); SSP group, and native spines. Vertical bars indicate SE ($n = 7$ in all group). Horizontal lines indicate significant differences (spinal fusion performed using stainless steel pins; $p < 0.05$).

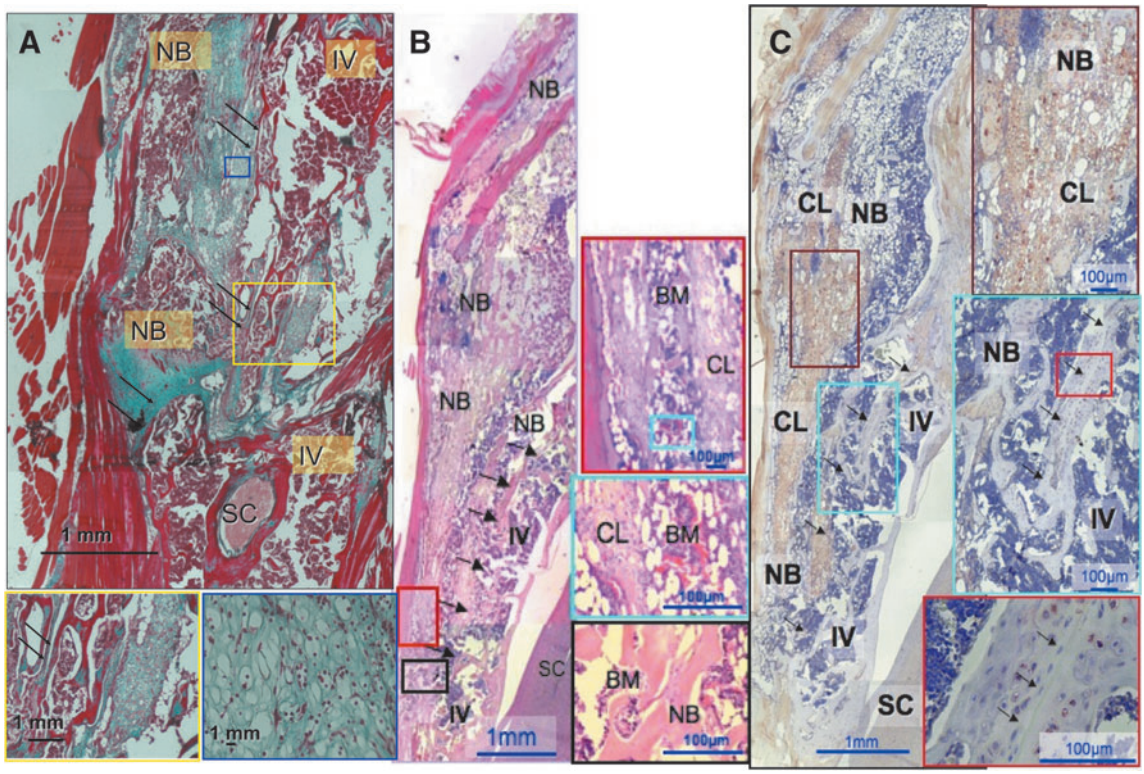

FIG. 6. Histological and immunohistochemical analysis of the newly formed bone. Histological analysis showed a fusion between the newly formed bone mass and the intact vertebra. Immunohistochemistry for β-*Gal* showed the presence of genetically engineered MSCs in the newly formed bone. (**A**) Hematoxylin and eosin standard staining; (**B**) Masson's Trichrome bone mass-specific staining; (**C**) immunohistochemical staining for β-*Gal*. Boxes show magnification of specific areas in the section. Arrows represent spinal fusion sites. IV, intact vertebra; NB, new bone; CL, cartilage-like tissue; SC, spinal cord; BM, bone marrow. Color images available online at www.liebertonline.com/ten.

genetically engineered MSCs to newly formed bone mass and resulting spinal fusion. The immunohistochemical findings showed that the newly formed bone contained numerous β-*Gal*-labeled MSCs (Fig. 6C). Positive staining appeared mainly in hypertrophic chondrocytes and in osteocytes embedded in the new bone tissue. No staining for β-*Gal* was visible in the native vertebra (Native Spine group), except at the site of fusion.

Discussion

MSCs are being extensively investigated for use in tissue regeneration. In the presence of a potent osteogenic inducer, such as BMP, MSCs can accelerate bone formation and lead to spine fusion. This can be achieved either by culturing MSCs in the presence of BMP and then transplanting them[35] or by overexpressing the gene encoding for BMP-2 in the implanted cells. The latter approach has the advantage of a sustained secretion of BMP *in vivo*, affecting both host and the implanted cells, in a synergistic autocrine/paracrine mechanism.[36] We have previously shown that BMP gene-modified MSCs secrete physiological quantities (nanograms) of BMP[28,34] over a period of few weeks compared to the mega doses used in rhBMP therapy (milligrams). Thus, the use of gene-modified MSCs might prevent recently described toxic side effects and inflammatory response induced by high doses of BMP[11,12]. In addition, gene modification could be applied to freshly isolated, noncultured MSCs[37] without the need for a cell culture phase. The use of noncultured MSCs could facilitate the translation of this therapeutic approach to the clinical arena. The present study marks the first time that the biomechanical properties of spinal fusion induced by injected genetically engineered MSCs have been evaluated. Before this study, we have only evaluated the morphometric and histological properties of the newly formed bone[28,38] and the nanomechanical and nanostructural properties of the engineered tissue.[26] The biomechanical tests that we performed represent a novel quantitative investigation of fusion integrity that enabled us to evaluate the quality of the spinal fusion and its clinical relevance.

Our findings demonstrate that the rigidity of spines fused using genetically engineered cells is similar to that of spines fused using bilateral stainless steel fixation across the vertebral processes; the MSC/+DOX and FG Only control groups exhibited significantly less rigidity, similar to those found in the Native Spine group. These findings show that the spinal fusion achieved using injections of genetically engineered MSCs can provide segmental stabilization of vertebrae without the need for an invasive surgical operation.

The structural properties of *de novo* bone tissue formation induced by genetically engineered MSCs were quantified using μCT. 3D μCT reconstructions of the spines demonstrated a bridge spanning 3.1 ± 0.6 vertebrae per mouse

($n = 9$) and 2.4 ± 0.4 vertebrae per injection ($n = 9$), although the bone tissue formed along the paraspinal muscle. The localization of spinal fusion in desired segments may be easier in a large animal model, because the choice of injection site in such a model can be more accurately controlled. In addition, we envision that in a large animal, multiple injections of stem cells will induce incremental bone tissue formation, increasing control over the site of tissue formation and spinal fusion.

In this study we also evaluated the relative contribution of the fused spine segments to the rigidity of the entire spine. Our findings demonstrated that the largest contribution came from the fused L3–L5 segment, corresponding to the site of the MSC injection and correlating to stainless steel pin-based fusion. When we examined the structural properties of the new bone formation, which we quantified using μCT, we found that the newly formed bone had a lower BVD and BMD than the posterolateral compartment of intact vertebra. These findings were probably due to the relatively short period of tissue formation, which is insufficient to create mature bone that can hold up to the same parameters as intact bone, which was used as a control (Native Spine group) in this study. On the other hand, when it comes to the structural parameters of the newly formed bone mass, such as DA and average BT, we found values similar to that of native vertebra. Further, the Conn-Den of new bone mass was greater than that in the control vertebra ($p < 0.05$), demonstrating that although not completely matured, the new bone has a branched structure that is sufficiently robust to enable a stable fusion.

Histological analyses of bone mass performed using standard H&E and Masson trichrome stains confirmed that the newly formed mass has typical morphological characteristics of bone, including cortex, trabeculae, and bone marrow. In addition, several cartilage-like islands were found inside the new bone formation, which probably represent cells that have not yet fully differentiated but will do so later and will contribute to the BVD and the strength of the tissue and fusion.

An immunohistochemical analysis was performed to detect engineered MSCs within the new bone mass. The assay showed that the newly formed bone contained cells that expressed β-*Gal*. Most of the positively stained cells were hypertrophic chondrocytes, whereas others were osteocytes embedded in new bone. Yet, it is hard to determine precisely using this method how much of the bone tissue was formed by the implanted cells compared to the contribution of host cells recruited to the region. However, it is safe to assume that both donor and host cells contributed to the new bone formation, given the paracrine action of the rhBMP-2 expressed by the MSCs, which would activate nearby host cells to differentiate into osteogenic cells.[28]

All these findings support and reinforce the value of our MSC-based treatment as a method of stabilizing vertebrae. The biomechanical data represent an essential proof of principle with regard to the functional stability of the fused vertebrae. Although biomechanical stabilization has been demonstrated, it is important to note that this approach involves heretrotopic ossification, which is not the current practice in the clinic today. Therefore, further examination of this model is needed in larger animal models. These future experiments will eventually allow us to advance the method to clinical trials and further evaluate the quality of MSC induced spinal fusion as a potential noninvasive technique for fixture of spinal vertebrae. We envision that in the future, the clinical application of this model to posterior and anterior spinal fusion will include fresh immunoisolated human MSCs[37] and that overexpression of BMP will be achieved via nonviral gene delivery[21,24] of MSCs shortly after their isolation. In summary, we presented here an injectable therapy for spine fusion that does not involve complex surgical procedures. In addition, the use of potent osteogenic cells could potentially replace the use of autografts that result in comorbidity at the donor site or allografts that have limited osteoinduction properties.

Acknowledgments

This study was partially supported by National Institutes of Health Grants No. R01AR056694-01A1 and R01DE019902-01 (D.G. and G.P.).

Disclosure Statement

No competing financial interests exist

References

1. Sobajima, S., Kim, J.S., Gilbertson, L.G., and Kang, J.D. Gene therapy for degenerative disc disease. Gene Ther **11,** 390, 2004.
2. Cassinelli, E.H., Hall, R.A., and Kang, J.D. Biochemistry of intervertebral disc degeneration and the potential for gene therapy applications. Spine J **1,** 205, 2001.
3. Kraemer, J. Natural course and prognosis of intervertebral disc diseases. International Society for the Study of the Lumbar Spine Seattle, Washington, June 1994. Spine **20,** 635, 1995.
4. Yoon, S.T., and Boden, S.D. Spine fusion by gene therapy. Gene Ther **11,** 360, 2004.
5. Wang, M.C., Chan, L., Maiman, D.J., Kreuter, W., and Deyo, R.A. Complications and mortality associated with cervical spine surgery for degenerative disease in the United States. Spine **32,** 342, 2007.
6. Kager, A.N., Marks, M., Bastrom, T., and Newton, P.O. Morbidity of iliac crest bone graft harvesting in adolescent deformity surgery. J Pediatr Orthop **26,** 132, 2006.
7. Swan, M.C., and Goodacre, T.E. Morbidity at the iliac crest donor site following bone grafting of the cleft alveolus. Br J Oral Maxillofac Surg **44,** 129, 2006.
8. Buttermann, G.R. Prospective nonrandomized comparison of an allograft with bone morphogenic protein versus an iliac-crest autograft in anterior cervical discectomy and fusion. Spine J **8,** 426, 2008.
9. Betz, R.R., Petrizzo, A.M., Kerner, P.J., Falatyn, S.P., Clements, D.H., and Huss, G.K. Allograft versus no graft with a posterior multisegmented hook system for the treatment of idiopathic scoliosis. Spine **31,** 121, 2006.
10. Fang, A., Hu, S.S., Endres, N., and Bradford, D.S. Risk factors for infection after spinal surgery. Spine **30,** 1460, 2005.
11. Chen, N.F., Smith, Z.A., Stiner, E., Armin, S., Sheikh, H., and Khoo, L.T. Symptomatic ectopic bone formation after off-label use of recombinant human bone morphogenetic protein-2 in transforaminal lumbar interbody fusion. J Neurosurg Spine **12,** 40, 2010.
12. Deutsch, H. High-dose bone morphogenetic protein-induced ectopic abdomen bone growth. Spine J **10,** e1, 2010.

13. Kim, D.H., and Vaccaro, A.R. Osteoporotic compression fractures of the spine; current options and considerations for treatment. Spine J **6,** 479, 2006.
14. Gibson, J.N., Grant, I.C., and Waddell, G. The Cochrane review of surgery for lumbar disc prolapse and degenerative lumbar spondylosis. Spine **24,** 1820, 1999.
15. Kim, H.S., Viggeswarapu, M., Boden, S.D., Liu, Y., Hair, G.A., Louis-Ugbo, J., Murakami, H., Minamide, A., Suh, D.Y., and Titus, L. Overcoming the immune response to permit *ex vivo* gene therapy for spine fusion with human type 5 adenoviral delivery of the LIM mineralization protein-1 cDNA. Spine **28,** 219, 2003.
16. Risbud, M.V., Shapiro, I.M., Guttapalli, A., Di Martino, A., Danielson, K.G., Beiner, J.M., Hillibrand, A., Albert, T.J., Anderson, D.G., and Vaccaro, A.R. Osteogenic potential of adult human stem cells of the lumbar vertebral body and the iliac crest. Spine **31,** 83, 2006.
17. Nakajima, T., Iizuka, H., Tsutsumi, S., Kayakabe, M., and Takagishi, K. Evaluation of posterolateral spinal fusion using mesenchymal stem cells: differences with or without osteogenic differentiation. Spine **32,** 2432, 2007.
18. Helm, G.A., and Gazit, Z. Future uses of mesenchymal stem cells in spine surgery. Neurosurg Focus **19,** E13, 2005.
19. Gan, Y., Dai, K., Zhang, P., Tang, T., Zhu, Z., and Lu, J. The clinical use of enriched bone marrow stem cells combined with porous beta-tricalcium phosphate in posterior spinal fusion. Biomaterials **29,** 3973, 2008.
20. Hasharoni, A., Zilberman, Y., Turgeman, G., Helm, G.A., Liebergall, M., and Gazit, D. Murine spinal fusion induced by engineered mesenchymal stem cells that conditionally express bone morphogenetic protein-2. J Neurosurg Spine **3,** 47, 2005.
21. Sheyn, D., Kimelman-Bleich, N., Pelled, G., Zilberman, Y., Gazit, D., and Gazit, Z. Ultrasound-based nonviral gene delivery induces bone formation *in vivo*. Gene Ther **15,** 257, 2008.
22. Dumont, R.J., Dayoub, H., Li, J.Z., Dumont, A.S., Kallmes, D.F., Hankins, G.R., and Helm, G.A. *Ex vivo* bone morphogenetic protein-9 gene therapy using human mesenchymal stem cells induces spinal fusion in rodents. Neurosurgery **51,** 1239, 2002.
23. Laurent, J.J., Webb, K.M., Beres, E.J., McGee, K., Li, J., van Rietbergen, B., and Helm, G.A. The use of bone morphogenetic protein-6 gene therapy for percutaneous spinal fusion in rabbits. J Neurosurg Spine **1,** 90, 2004.
24. Aslan, H., Zilberman, Y., Arbeli, V., Sheyn, D., Matan, Y., Liebergall, M., Zhong, J., Helm, G.A., Gazit, D., and Gazit, Z. Nucleofection-based *ex vivo* nonviral gene delivery to human stem cells as a platform for tissue regeneration. Tissue Eng **12,** 877 2006.
25. Zuk, P.A., Zhu, M., Ashjian, P., De Ugarte, D.A., Huang, J.I., Mizuno, H., Alfonso, Z.C., Fraser, J.K., Benhaim, P., and Hedrick, M.H. Human adipose tissue is a source of multipotent stem cells. Mol Biol Cell **13,** 4279, 2002.
26. Pelled, G., Tai, K., Sheyn, D., Zilberman, Y., Kumbar, S., Nair, L.S., Laurencin, C.T., Gazit, D., and Ortiz, C. Structural and nanoindentation studies of stem cell-based tissue-engineered bone. J Biomech **40,** 399, 2007.
27. Tai, K., Pelled, G., Sheyn, D., Bershteyn, A., Han, L., Kallai, I., Zilberman, Y., Ortiz, C., and Gazit, D. Nanobiomechanics of repair bone regenerated by genetically modified mesenchymal stem cells. Tissue Eng Part A **14,** 1709, 2008.
28. Moutsatsos, I.K., Turgeman, G., Zhou, S., Kurkalli, B.G., Pelled, G., Tzur, L., Kelley, P., Stumm, N., Mi, S., Muller, R., Zilberman, Y., and Gazit, D. Exogenously regulated stem cell-mediated gene therapy for bone regeneration. Mol Ther **3,** 449, 2001.
29. Hildebrand, T., Laib, A., Muller, R., Dequeker, J., and Ruegsegger, P. Direct three-dimensional morphometric analysis of human cancellous bone: microstructural data from spine, femur, iliac crest, and calcaneus. J Bone Miner Res **14,** 1167, 1999.
30. Muller, R., Hildebrand, T., and Ruegsegger, P. Non-invasive bone biopsy: a new method to analyse and display the three-dimensional structure of trabecular bone. Phys Med Biol **39,** 145, 1994.
31. ASTM. Standard Test Method for Flexural Properties of Unreinforced and Reinforced Plastics and Electrical Insulating Materials by Four-Point Bending. D6272. ASTM, 2002, p. 519.
32. Cottrell, J.M., van der Meulen, M.C., Lane, J.M., and Myers, E.R. Assessing the stiffness of spinal fusion in animal models. HSS J **2,** 12, 2006.
33. Beer, F.P., Johnston, E.R., and DeWolf, J.T. Mechanics of Materials. Burr Ridge, IL: McGraw-Hill Higher Education, 2006.
34. Turgeman, G., Pittman, D.D., Muller, R., Kurkalli, B.G., Zhou, S., Pelled, G., Peyser, A., Zilberman, Y., Moutsatsos, I.K., and Gazit, D. Engineered human mesenchymal stem cells: a novel platform for skeletal cell mediated gene therapy. J Gene Med **3,** 240, 2001.
35. Fu, T.S., Chen, W.J., Chen, L.H., Lin, S.S., Liu, S.J., and Ueng, S.W. Enhancement of posterolateral lumbar spine fusion using low-dose rhBMP-2 and cultured marrow stromal cells. J Orthop Res **27,** 380, 2009.
36. Gazit, D., Turgeman, G., Kelley, P., Wang, E., Jalenak, M., Zilberman, Y., and Moutsatsos, I. Engineered pluripotent mesenchymal cells integrate and differentiate in regenerating bone: a novel cell-mediated gene therapy. J Gene Med **1,** 121, 1999.
37. Aslan, H., Zilberman, Y., Kandel, L., Liebergall, M., Oskouian, R.J., Gazit, D., and Gazit, Z. Osteogenic differentiation of noncultured immunoisolated bone marrow-derived CD105+ cells. Stem Cells **24,** 1728, 2006.
38. Sheyn, D., Pelled, G., Zilberman, Y., Talasazan, F., Frank, J.M., Gazit, D., and Gazit, Z. Nonvirally engineered porcine adipose tissue-derived stem cells: use in posterior spinal fusion. Stem Cells **26,** 1056, 2008.

Address correspondence to:
Dan Gazit, D.M.D., Ph.D.
Hebrew University-Hadassah Dental Medicine Faculty
P.O. Box 12272
Ein Kerem, Jerusalem 91120
Israel

E-mail: dgaz@cc.huji.ac.il

Received: December 08, 2009
Accepted: July 09, 2010
Online Publication Date: September 16, 2010